

ERL-0162-TM

AR-002-041



DEPARTMENT OF DEFENCE

DEFENCE SCIENCE AND TECHNOLOGY ORGANISATION

ELECTRONICS RESEARCH LABORATORY

DEFENCE RESEARCH CENTRE SALISBURY
SOUTH AUSTRALIA

TECHNICAL MEMORANDUM

ERL-0162-TM

AN ASSESSMENT OF THE CROSSED PORRO PRISM RESONATOR

B.A. SEE, R. SEYMOUR and K. FUELOEP



DTIC
ELECTE
MAR 19 1981

A

Approved for Public Release

AUGUST 1980

COPY No. 12

AD A 096538

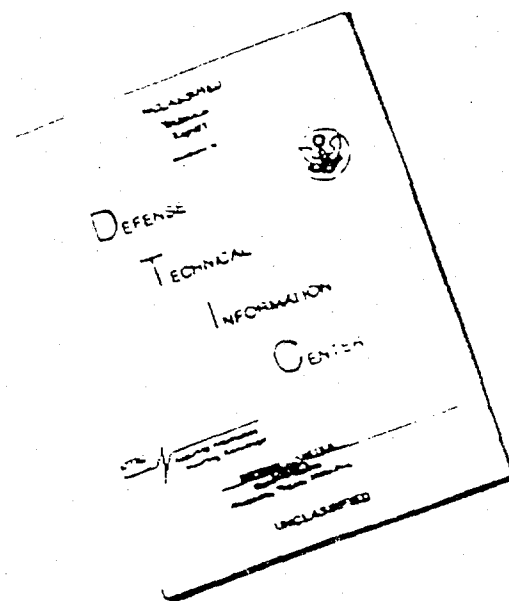
DAS FILE COPY

12

TW

TW

DISCLAIMER NOTICE



THIS DOCUMENT IS BEST QUALITY AVAILABLE. THE COPY FURNISHED TO DTIC CONTAINED A SIGNIFICANT NUMBER OF PAGES WHICH DO NOT REPRODUCE LEGIBLY.

UNCLASSIFIED

AR-002-041

DEPARTMENT OF DEFENCE
DEFENCE SCIENCE AND TECHNOLOGY ORGANISATION
ELECTRONICS RESEARCH LABORATORY

9 TECHNICAL MEMORANDUM
141 ERL-0162-TM

6 AN ASSESSMENT OF THE CROSSED PORRO PRISM RESONATOR.

101 B.A. See K. Fueleop and R. Seymour

11 Aug 80

SUMMARY

12 38

Lasers with Crossed Porro Prism Resonators are in production in both the USA and the UK for military laser rangefinder and designator applications.

This paper reviews the properties of these devices and examines the advantages over normal mirror resonators.

The theory of operation is treated in this paper and the mechanical stability and other features of the laser are examined and compared to standard mirror resonators.



POSTAL ADDRESS: Chief Superintendent, Electronics Research Laboratory,
Box 2151, GPO, Adelaide, South Australia, 5001.

UNCLASSIFIED

410863

DM

DOCUMENT CONTROL DATA SHEET

Security classification of this page

UNCLASSIFIED

<p>1 DOCUMENT NUMBERS</p> <p>AR Number: AR-002-041</p> <p>Report Number: ERL-0162-TM</p> <p>Other Numbers:</p>	<p>2 SECURITY CLASSIFICATION</p> <p>a. Complete Document: Unclassified</p> <p>b. Title in Isolation: Unclassified</p> <p>c. Summary in Isolation: Unclassified</p>
--	---

3 TITLE

AN ASSESSMENT OF THE CROSSED PORRO RESONATOR

<p>4 PERSONAL AUTHOR(S):</p> <p>B.A. See, K. Fuloep and R. Seymour</p>	<p>5 DOCUMENT DATE:</p> <p>August 1980</p>
--	--

6 6.1 TOTAL NUMBER OF PAGES 16

6.2 NUMBER OF REFERENCES: 13

<p>7 7.1 CORPORATE AUTHOR(S):</p> <p>Electronic Research Laboratory</p> <p>7.2 DOCUMENT SERIES AND NUMBER</p> <p>Electronics Research Laboratory 0162-TM</p>	<p>8 REFERENCE NUMBERS</p> <p>a. Task: 79/049</p> <p>b. Sponsoring Agency: Defence</p>
--	--

9 COST CODE:

217599

<p>10 IMPRINT (Publishing organisation)</p> <p>Defence Research Centre Salisbury</p>	<p>11 COMPUTER PROGRAM(S) (Title(s) and language(s))</p>
--	--

12 RELEASE LIMITATIONS (of the document):

Approved for Public Release

12.0	OVERSEAS	NO	P.R. 1	A	B	C	D	E
------	----------	----	--------	---	---	---	---	---

Security classification of this page:

UNCLASSIFIED

TABLE OF CONTENTS

	Page No.
1. INTRODUCTION	1
2. THEORY OF OPERATION	1
2.1 Output Coupling	1
2.2 Q Switch Azimuth Fixed	2
2.3 Q Switch Azimuth 45°	3
2.4 Axes Crossed	5
2.5 General Azimuth Angles	6
3. SELECTION OF MATERIALS	7
4. ANGULAR ALIGNMENT TOLERANCE	8
4.1 The Conventional Laser	9
4.2 The Crossed Porro Resonator	9
4.2.1 Roof Edges at 90°	10
4.2.2 Roof Edges at angle ψ	10
5. MEASUREMENT OF TOLERANCES	11
6. STANDING WAVE POWER DENSITY	12
7. SMOOTHING OF HOT SPOTS	13
8. CONCLUSION AND RECOMMENDATIONS	13
9. ACKNOWLEDGEMENTS	14
REFERENCES	15

LIST OF APPENDICES

I THE JONES CALCULUS	16
II PROGRAM FOR TI 59 PHASE SHIFT, COUPLING AND EXTINCTION RATIO	17

LIST OF FIGURES

1. In line and folded crossed porro resonators
2. Reflection of light ray in a porro prism
3. Output coupling versus azimuth angle
4. Extinction ratio with applied bias
5. Phase shift to shut Q switch
6. Feedback intensity vs. phase shift
7. Extinction ratio vs. refractive index
8. Extinction ratios for fused silica porro
9. Conventional Fabry-Perot resonator
10. Conventional resonator sensitivity
11. Porro prism tilted in its insensitive direction
12. Porro prism tilted in its sensitive direction
13. Projected view of optical axis displacement for porro prism
14. Relative output vs. porro misalignment
15. Relative output vs roof edge displacement
16. Beam intensities in resonators
17. Ray path rotation in crossed porro resonator
18. Elliptically polarised light ray

1. INTRODUCTION

Laser rangefinders and designators are currently entering the inventory of the Australian Defence Forces. At present the majority of such devices utilise Nd:YAIG lasers.

Weapons Systems Research Laboratory is studying laser designation systems and Advanced Engineering Laboratory has recently performed a feasibility study of a laser rangefinder for the RAAF(ref.1).

This report has been prepared in response to the requirements of the above tasks and to update laser expertise and assess whether the crossed porro technique has any advantages in a high repetition rate (168 Hz) laser for the laser depth sounder system under development in Electronics Research Laboratory.

The name "Crossed Porro Resonator" infers that the two roof edges make an angle of 90°, this is not always the case; in general the angle between the roof edges may be other than 90° but the arrangement is still called a Crossed Porro Resonator.

2. THEORY OF OPERATION

2.1 Output Coupling

The theory of operation of the crossed porro resonator has been treated by a number of authors(ref.2,3) and in most detail by Chun and Teppo(ref.4) .

In figure 1, two possible laser configurations are shown. Figure 1(a) shows an in line system with output from the side and figure 1(b) a folded system with in line output. These configurations are as shown in references 5 and 6.

In figure 2, a light ray is incident on a porro prism whose roof edge makes an azimuth angle ϕ to the horizontal. There is a differential phase shift between the parallel and perpendicular components(ref.7,8) of

$$\delta = \delta_1 - \delta_2$$

on each reflection,

where

$$\delta_1 = 2 \tan^{-1} \{ [n \sqrt{(n^2 \sin^2 \phi - 1)}] / \cos \phi \}$$

$$\delta_2 = 2 \tan^{-1} \{ [n^2 \sin^2 \phi - 1] / [n \cos \phi] \}$$

ϕ being the angle of incidence on the rear face of the porro prism and n the refractive index.

The parallel component is inverted by the reflection while the perpendicular component is not, see figure 2. The total phase shift due to the two reflections becomes

$$P = \pi + 4 \tan^{-1} \{ [\sqrt{(\sin^2 \phi - n^{-2})} \cos \phi] / \sin^2 \phi \}$$

and since ϕ = 45°, the phase shift reduces to

$$P = \pi + 4 \tan^{-1} \{ \sqrt{[1 - 2/(n^2)]} \}$$

In the laser, the plane polarised beam from the polarising beam splitter

will, on emerging from the porro, be elliptically polarised and a component will then be rejected by the polariser constituting the output.

The magnitude of the coupling can be determined using Jones calculus(ref.9), the essential features of which are given in Appendix 1. For the folded system shown in figure 1(b) the light incident on the porro prism is vertically polarised; the light reflected back to the polariser can then be represented by

$$\begin{Bmatrix} A_x \exp(i\varepsilon_x) \\ A_y \exp(i\varepsilon_y) \end{Bmatrix} = M_p \begin{Bmatrix} 0 \\ 1 \end{Bmatrix}$$

where M_p is the porro retardation matrix.

$$M_p(\delta_p, \rho_p) = \begin{Bmatrix} \cos(\delta_p/2) + i \sin(\delta_p/2) \cos(2\rho_p) & i \sin(\delta_p/2) \sin(2\rho_p) \\ i \sin(\delta_p/2) \sin(2\rho_p) & \cos(\delta_p/2) - i \sin(\delta_p/2) \cos(2\rho_p) \end{Bmatrix}$$

The subscript p refers to the porro prism, δ_p is the total phase shift (P) and ρ_p is the porro prism azimuth angle.

The transmitted component (X component) constitutes the output. The intensity of the output is

$$(A_x)^2 = \sin^2(\delta_p/2) \sin^2(2\rho_p)$$

In Chun and Teppo a plot is shown of out-coupling reflectivity against azimuth angle. In their work the term "out-coupling reflectivity" means feedback. For in-line operation, figure 1(a), the horizontally polarised component constitutes the feedback while the vertical constitutes the output.

Figure 3 is a plot of output against prism azimuth angle for some commonly available materials. Note that the highest output is obtained for low index materials where the phase shift P approaches π .

2.2 Q Switch Azimuth Fixed

Referring again to figure 1(b), the beam returning to the polariser after going through the Q switch-Porro-Q switch train can be written

$$\begin{Bmatrix} A_x \exp(i\varepsilon_x) \\ A_y \exp(i\varepsilon_y) \end{Bmatrix} = Q M Q \begin{Bmatrix} 0 \\ 1 \end{Bmatrix}$$

where M is the porro matrix and the Q switch matrix is

$$Q(\delta_q, \rho_q) = \begin{Bmatrix} \cos(\delta_q/2) + i \sin(\delta_q/2) \cos(2\rho_q) & i \sin(\delta_q/2) \sin(2\rho_q) \\ i \sin(\delta_q/2) \sin(2\rho_q) & \cos(\delta_q/2) - i \sin(\delta_q/2) \cos(2\rho_q) \end{Bmatrix}$$

Putting

$$A = \cos(\delta_p/2) + i \sin(\delta_p/2)\cos(2\rho_p)$$

$$B = \sin(\delta_p/2)\sin(2\rho_p)$$

$$C = \cos(\delta_q/2) + i \sin(\delta_q/2)\cos(2\rho_q)$$

$$S = \sin(\delta_q/2)\sin(2\rho_q)$$

the emerging beam can be obtained as

$$\begin{Bmatrix} A_x \exp(i \epsilon_x) \\ A_y \exp(i \epsilon_y) \end{Bmatrix} = Q M Q \begin{Bmatrix} 0 \\ 1 \end{Bmatrix}$$

$$= \begin{Bmatrix} i [B C C^* - B S^2 + A S C + A^* S C^*] \\ [A^* C^{*2} - 2 B C^* S - A S^2] \end{Bmatrix}$$

The Y component is in general complex and has components which when written out explicitly are

$$\text{Re}(A_y) = \cos(\delta_p/2)\cos(\delta_q) - \sin(\delta_p/2)\sin(\delta_q)\cos(2\rho)$$

$$\text{Im}(A_y) = [\sin(\delta_p/2)\cos(\delta_q)\cos(2\rho) + \cos(\delta_p/2)\sin(\delta_q)]\cos(2\rho_q) - \sin(\delta_p/2)\sin(2\rho)\sin(2\rho_q)$$

where $\rho = \rho_p - \rho_q$

The X component is however purely imaginary in all cases and is given by

$$A_x = i \{ [\sin(\delta_p/2)\cos(\delta_q)\cos(2\rho) + \cos(\delta_p/2)\sin(\delta_q)]\sin(2\rho_q) + \sin(\delta_p/2)\sin(2\rho)\cos(2\rho_q) \}$$

When the Q switch is open, the X component should vanish and the Y component should be of unit intensity. When the Q switch is shut, the X component should be of unit intensity but the Y component should vanish.

In the following sections we consider first some special cases of azimuth angles of particular practical interest and then return to the general case in Section 2.5.

2.3 Q Switch Azimuth 45°

In practice it is convenient to hold the Q switch azimuth fixed at $\rho = \pm 45^\circ$; we now take $\rho = -45^\circ$. For the Q switch open, the condition $A_x = 0$ leads to

$$\tan \delta_q = \tan(\delta_p/2)\sin(2\rho_p)$$

If $\rho_p = +45^\circ$, i.e. the Q switch and prism axes are crossed,

$$\delta_q = \delta_p/2.$$

For the Q switch shut, the condition $|A_x| = 1$ leads to

$$\sin(\delta_p/2)\cos(\delta_q)\sin(2\rho_p) - \cos(\delta_p/2)\sin(\delta_q) = 1$$

Now if $\rho_p = +45^\circ$, ie axes crossed

$$\sin[(\delta_p/2) - \delta_q] = \pm 1$$

or $\delta_q = \delta_p/2 \pm \pi/2$

The phase shift required for the Q switch in the shut condition differs by 90° from the open condition as indeed it should. For the Q switch shut and ρ_p other than 45° we make use of the phase shift obtained for the open condition to obtain the phase shift required to close the Q switch.

Since $(\delta_q)_{\text{open}} = \tan^{-1}[\tan(\delta_p/2)\sin(2\rho_p)]$

then $(\delta_q)_{\text{shut}} = (\delta_q)_{\text{open}} \pm \pi/2$

In obtaining this result, only the X component has been considered. Evaluation of the Y component shows that

$$|A_y| = 1 \quad \text{for the Q switch open}$$

but $|A_y| \neq 0$ for the Q switch shut unless $\rho_p = \pm 45^\circ$.

Hence the extinction ratio is limited for any prism azimuth angle other than $\rho_p = \pm 45^\circ$.

Since the extinction ratio is the ratio of maximum to minimum transmitted intensity of the Y component, it can be written as

$$\text{Extinction Ratio} = 1/[(A_y)^2]$$

where A_y is the transmitted component with the Q switch shut. The

extinction ratio and phase shift required can be computed with the aid of the preceding formulae. A program listing for a TI 59 hand calculator is given in Appendix II.

The extinction ratio is shown in figure 4 for some common materials and the phase shift required to shut the Q switch in figure 5. Note that in figure 4 the highest extinction ratio is obtained for high index materials, the converse of the result of Chun and Teppo (their figure 4). It is believed their curves have been incorrectly labelled.

The result obtained here is easily verified by considering the phase shifts involved. If the Q switch phase shift is $\pi/2$, then two passages through the Q switch give a phase shift of π , making the polarisation emerge at right angles to the incident polarisation. To preserve this situation a phase shift of 0 or 2π is required in the prism. Since as previously stated the prism phase shift

$$P = \pi + 4\tan^{-1}\{ \sqrt{[1 - 2/(n^2)] } \}$$

then $P \longrightarrow 2\pi$ as $n \longrightarrow \infty$

As n approaches $\sqrt{2}$, P tends to π and the total phase shift tends to 2π leaving the emerging polarisation the same as the incident polarisation,

that is the Q switch is partially open giving a low extinction ratio. It should also be noted that the extinction ratio of figure 4 refers to the case of bias being applied to the Q switch.

In figure 6, the intensity of the feedback component is plotted against the Q switch phase shift for azimuth angles of 15° , 30° and 45° for a fused silica porro. In the open state $(A_y)^2 = 1$ for any azimuth angle while for the Q switch shut leakage occurs for any azimuth angle other than 45° . If no bias is applied, ie $\delta_q = 0$, the extinction ratio is determined solely by the feedback component due to the prism.

$$\begin{aligned} \text{Ext. Ratio} &= \{ (A_y)^2 \}^{-1} \\ \text{(no bias)} &= \{ [\cos^2(\delta_p/2) + \sin^2(\delta_p/2) \cos^2(2\rho_p)]^{-1} \} \end{aligned}$$

and this is finite even for $\rho_p = \pm 45^\circ$, in which case

$$\begin{aligned} \text{Ext. Ratio} &= \{ \cos^2(\delta_p/2) \}^{-1} \\ \text{(no bias)} & \end{aligned}$$

In this case a higher extinction ratio is obtained with low index materials since no phase shift occurs in the Q switch and the total phase shift derived from the prism

$$P \longrightarrow \pi \quad \text{as} \quad n \longrightarrow \sqrt{2}.$$

The extinction ratio without bias for $\rho_p = 45^\circ$ is plotted in figure 7

as a function of refractive index. To achieve an extinction ratio of better than 10:1 an index of < 1.433 is required.

2.4 Axes Crossed

As an additional special case we consider both Q switch and porro azimuths variable but restricted such that their axes remain crossed

$$\text{ie } \rho = \rho_p - \rho_q = 90^\circ$$

Here the Q switch open condition, $A_x = 0$, leads to

$$A_x = i \sin(\delta_q - \delta_p/2) \sin(2\rho_q) = 0$$

which is satisfied at $\delta_q = \delta_p/2$, as in Section 2.3 when the axes were crossed ($\rho_q = -45^\circ$ and $\rho_p = +45^\circ$).

With the condition $\rho = 90^\circ$, A_y is

$$A_y = \cos(\delta_q - \delta_p/2) + i \sin(\delta_q - \delta_p/2) \cos(2\rho_q)$$

and $|A_y|$ is never zero, but attains its minimum value of $\cos^2(2\rho_q)$

at the expected Q switch shut condition of

$$\delta_q = \delta_p/2 + \pi/2$$

The extinction ratio in this case is

$$\begin{aligned} \text{Ext. Ratio} &= [(A_y)^{-2}] \\ &= [\cos^{-2} 2\rho_q] \end{aligned}$$

Since in this instance $\rho_p = \rho_q + \pi/2$, an infinite extinction ratio can only be obtained if both prism and Q switch azimuth angles are $\pm 45^\circ$.

The extinction ratio with and without bias for $\rho_q = -45^\circ$ and the extinction ratio for $\rho_p = \rho_q + \pi/2$ are shown in figure 8 for a fused silica porro prism as a function of porro prism azimuth. Best extinction is obtained with $\rho_q = -45^\circ$, for any porro azimuth.

2.5 General Azimuth Angles

The general case is developed further here to determine whether an infinite extinction ratio can be obtained if the azimuth angles are not restricted. To obtain a zero value of $|A_y|$ it is necessary and sufficient

for both real and imaginary parts of A_y to be zero separately.

From Section 2.3, $\text{Re}(A_y) = 0$ requires

$$\cos(2\rho) = \cot(\delta_p/2)\cot(\delta_q)$$

For $\text{Im}(A_y)$ to be zero as well requires in addition that

$$\tan(2\rho_q) = \cos(\delta_q)\cot(2\rho) + \sin(\delta_q)\cos(\delta_p/2)/\sin(2\rho)$$

and hence a combined requirement is

$$\sin(2\rho_q) = \cos(\delta_p/2) / \sin(\delta_q)$$

It is thus possible to obtain infinite extinction for a wide range of values of δ_q , ρ_q and ρ_p for a given porro phase shift δ_p .

The restriction $\rho = \pi/2$ and $\rho_q = \pm 45^\circ$ is not necessary for infinite extinction and δ_q can range from $\delta_p/2 - \pi/2$ to $\delta_p/2 + \pi/2$.

This range does not include $\delta_q = 0$ and hence it is not possible to obtain

infinite extinction for zero phase shift of the Q switch, but since a Lithium Niobate Q switch cut along a naturally birefringent direction has non-zero phase shift for zero voltage and it should be possible to select crystal lengths such that, using the preceding formulae, azimuth angles can be found to give infinite extinction at zero voltage.

It is of interest that infinite extinction can be obtained at $\delta_q = \pi/2$ for the values of $\rho = \pi/4$, $\rho_q = (\delta_p - \pi)/4$, and $\rho_p = (\delta_p + \pi)/4$. However when $\delta_q = 0$ (Q switch nominally open) with these azimuth angles we obtain for the Y component

$$|A_y|^2 = 1 - \sin^4(\delta_p/2)$$

and the Q switch is thus not fully open. A similar result is obtained in the general case. If a value of δ_q , say δ_0 , together with values ρ and ρ_q are found which satisfy the conditions for infinite extinction, then at the same azimuth angles but different ρ_q , A_y can be written

$$\begin{aligned} \text{Re}(A_y) &= \sin(2\rho_q)\sin(\delta_0 - \delta_q) \\ \text{Im}(A_y) &= \sin(2\rho_q)\cos(2\rho_q)[\cos(\delta_q - \delta_0) - 1] \end{aligned}$$

$|A_y|^2$ thus has a maximum value at $\delta_q = \delta_0 + \pi/2$ but this value is

$$|A_y|^2 = 1 - \cos^4(2\rho_q)$$

It must be concluded that although it is possible to obtain infinite extinction at a range of values of δ_q by selection of the unique azimuth angles, it is not possible to completely open the Q switch at these same azimuth angles. Conversely it is possible at all values of δ_q to find azimuth angles related by the condition $A_x = 0$, to completely open the Q switch but infinite extinction cannot be obtained for these azimuth angles. Only at the angles $\rho_p = \pm 45^\circ$ and $\rho_q = \pm 45^\circ$ is it possible to completely open and completely close the Q switch.

3. SELECTION OF MATERIALS

The selection of the optical materials for fabrication of the porro prisms is influenced by the output energy required and whether or not one wishes to provide bias on the Q switch. If no bias is provided then the extinction ratio is limited by the porro prism as we have seen in Section 2.3. In this case fused silica is a good choice since its index of refraction is low ($n = 1.4496$).

The extinction ratio for $\rho_p = 45^\circ$ is then

$$\text{Ext. Ratio} = 5.7 : 1$$

Further hold-off is provided by the coupling porro. If this is also fused silica then threshold in the laser will occur when

$$[G_o (1 - C)] = 1.$$

Here $G_o = \exp(g_o l)$

where g_o is the small signal gain coefficient, l is the length of the rod and C is the coupling of the porros. For silica $C = 0.82$ at $\rho_p = 45^\circ$, giving

$$G_o = 1/(1-C) = 5.56$$

also $g_o = \beta \cdot E_{st}$

but for Nd:YAlG(ref.10)

$$\beta = 4.73 \text{ cm}^2/\text{J}$$

and E_{st} is the stored energy per unit volume. Then

$$\beta \cdot E_{st} \cdot l = \ln(5.56) = 1.714$$

and $E_{st} = 0.362/l \text{ J/cm}^3$

The total stored energy is

$$E_{st} \cdot V = 0.284 D^2 \text{ Joule}$$

where D is the rod diameter in centimetres and V the rod volume. Hence the total stored energy at threshold for a 6 mm diameter rod is

$$E_{st} \cdot V = 0.102 \text{ Joule}$$

Thus without bias on the Q switch a Nd:YAlG laser can operate up to 100 mj output. Above this value bias would need to be provided on the Q switch.

If bias is to be provided then a silica porro can still be used but a higher index material would in this case give a higher extinction ratio.

For the coupling porro, silica is a good choice as it allows the coupling to be optimised in the range 0 to 80% by adjusting the azimuth angle. If it is desired to keep the azimuth angle near $\pm 45^\circ$ use of a higher index material will give reduced coupling, eg ED-4 will give a maximum of 54% coupling.

Other factors may influence the choice of materials such as the requirement to match thermal expansion coefficients to avoid optical strain birefringence when bonding components to mounts.

In their patent(ref.5) Ferranti fix the azimuth angles at $\pm 45^\circ$ and the desired coupling and biasing arrangements are achieved by selection of materials in conjunction with thin film coatings on the reflecting surfaces to modify the phase shift occurring on total internal reflection.

To achieve higher extinction ratios without bias one would need materials with lower refractive index. This may be achieved by coatings on the surfaces.

The modification of the phase shift with thin film coatings is discussed in references 11 and 12.

4. ANGULAR ALIGNMENT TOLERANCE

4.1 The Conventional Laser

In figure 9, a schematic of a conventional Q switched Nd:YAlG laser is shown. Output is taken via a partially transmitting mirror whose transmission is selected to be optimum at a given pump energy. The mirror transmission is normally in the range 50% to 80%.

The mechanical stability and sensitivity of the Fabry-Perot interferometer have been well documented(ref.10). For the resonator of figure 9, the optical axis of the system must be normal to both mirrors and pass through the centres of curvature. If one mirror is tilted, laser action will cease altogether when the optical axis coincides with the edge of the aperture of the laser rod. This is shown in figure 10(a) where the rod is assumed short and centrally located. From figure 10(a), the displacements of the optical axis are

$$\Delta_3 = (R_1 + R_2 - d)\phi = R_1\theta$$

$$\Delta_2 = R_2\phi$$

$$\Delta_1 = (R_1 - d)\phi$$

which can be rewritten as

$$\Delta_1 = \frac{R_1 (R_2 - d) \theta}{(R_1 + R_2 - d)}$$

$$\Delta_2 = \frac{R_1 R_2 \theta}{(R_1 + R_2 - d)}$$

For a typical case $R_1 = R_2 = 10\text{m}$, and for $d \ll R$, these become

$$\Delta_1 = \Delta_2 \cong (R\theta)/2.$$

When for example the displacement $\Delta = D/2$, where D is the rod diameter,

$$\theta = D/R$$

and for $D = 5\text{ mm}$, $\theta = 0.5\text{ mrad}$.
 $= 102\text{ s of arc}$

of mirror misalignment (from Koehner, ref.10) and the above calculation is in good agreement with case (c) of the figure.

If the mirror radius is reduced the angular tolerance can be improved but at the expense of beam divergence which increases.

4.2 The Crossed Porro Resonator

The porro prism acts as a retroreflector which is sensitive to tilt about an axis perpendicular to the roof edge, but insensitive to tilt about the roof edge within the limits imposed by total internal reflection. Figure 11 is a side view of a porro prism tilted about the roof edge (greatly exaggerated).

The internal reflections occur at angles

$$\psi_1 = \pi/4 + \phi_r$$

$$\psi_2 = \pi/4 - \phi_r$$

where ϕ_r is the refraction angle. For small angles

$$\phi_r \cong \phi_i/n$$

where ϕ_i is the external angle of incidence (the tilt angle).

Provided ψ_2 is greater than the critical angle (ϕ_c), the incident ray is totally internally reflected back along a parallel path.

For $\psi_2 = \phi_c$ one obtains

$$\phi_i \cong n - \sqrt{2}$$

The tilt tolerance in this insensitive direction is thus directly related to refractive index. As n approaches $\sqrt{2}$ the tilt tolerance approaches zero.

In a crossed porro resonator, tilt of one prism in its sensitive direction can be compensated by the other because of this property.

For fused silica ($n = 1.4496$ at 1064 nm)

$$\phi_i \cong 2.03^\circ$$

4.2.1 Roof Edges at 90°

In figure 12 a misaligned cross porro resonator is shown with one porro tilted in its sensitive direction. For a stable system the axis of the system must pass through the apex of each prism. Figure 13(a) depicts a projected end on view of this with prism 1 tilted by θ about an axis parallel to roof edge 2. If the rod is centred and is short compared to the resonator length (d), the tilt angle needed to completely suppress laser action is

$$\theta = D/d$$

For $D = 5$ mm and $d = 30$ cm, the corresponding angle is

$$\begin{aligned} \theta &= 16.7 \text{ mrad} \\ &\cong 1 \text{ degree} \end{aligned}$$

When compared to the result obtained for the long radius mirror configuration it is seen that the crossed porro resonator is some 34 times less sensitive to angular misalignment.

4.2.2 Roof Edges at angle ψ

Figure 13(b) depicts the projected end view of the optical axis displacement when the prism roof edges make an angle ψ . Tilting prism 1 about an axis at right angles to its roof edge now results in displacement of the optical axis on both roof edges. The displacement at right angles to roof edge 2 is still

$$\Delta = d \theta$$

The total displacement

$$\Delta' = \Delta / \sin\psi = (d\theta) / \sin\psi$$

Again if the rod is short compared to the resonator length and is centrally located, then laser action will cease when

$$\Delta' = D/2 = (d\theta) / 2\sin\psi$$

or
$$\theta = (D\sin\psi) / d$$

Thus the tilt tolerance is reduced by the factor $\sin\psi$ when the porro prism roof edges make an angle of ψ . In the case previously considered the maximum tilt drops from 1° to $42'$ of arc for $\psi = 45^\circ$.

In Section 3 it was pointed out that without bias on the Q switch higher extinction ratios could be obtained for low index materials. It has been shown above that the tilt tolerance in the insensitive direction is directly related to refractive index, thus there would be little point in using an effective index < 1.432 since the external tilt tolerance in the insensitive direction would then be 1° , similar to the tilt tolerance in the sensitive direction.

5. MEASUREMENT OF TOLERANCES

A pair of commercial LANSING mounts with axial rotation were fitted with adapters which held the porro prisms and provided translation of the roof edge at right angles to the optical axis.

These allowed the following adjustments of the porro prisms :

- (a) Rotation in the insensitive direction, about the roof edge.
- (b) Rotation in the sensitive direction, about an axis at right angles to the roof edge.
- (c) Rotation of the porros about the optical axis, ie adjustment of the azimuth angle.
- (d) Translation of the roof edge to centre it on the optical axis.

There was no requirement in this experiment to measure the actual energy output of the laser, but rather to study the change of energy with respect to the mis-alignment of the porro prisms. The relative pulse energy was monitored by passing the output of the laser to a diffuser and thence to a silicon photo-diode, the output of which was displayed on an oscilloscope.

The linear displacements of the micrometers providing the tilt adjustments were converted to angular displacements via an appropriate constant and the azimuth angle read directly off a ring calibrated in two degree increments. Linear displacement of the roof edge was measured with vernier calipers using the optical bench as one reference and the edge of the prism holder as the other.

A set of three readings were taken for each degree of freedom and plotted. Optical elements were aligned in the usual manner. The laser was operated at 9 J pump energy and at a 10 Hz repetition rate. The output was peaked dynamically to obtain a reference set of micrometer readings.

The pulse amplitude displayed on the CRO was recorded as a function of angular displacement in both sensitive and insensitive directions for each prism in turn. After again peaking the output, the prism roof edges were displaced incrementally and the pulse amplitude recorded as a function of displacement.

All measurements were repeated several times and averaged.

In figure 14 the amplitude is plotted as a function of tilt in the insensitive direction. This is simply related to the critical angle for total internal reflection occurring in the prism. For the silica porros used tilt of up to 2° caused no change in output. Figure 14 also shows the relative pulse amplitude as a function of tilt in the sensitive direction. Misalignment of up to 10 minutes of arc causes a drop of less than 10%. By comparison the conventional resonator typically suffers a drop of 10% with a tilt of 10 s of arc (see figure 10(b)).

Figure 15 shows the relative pulse amplitude against linear displacement of the roof edge. A displacement of 0.25 mm can be tolerated without incurring significant drop in the output. Location of the roof edge to this accuracy should be possible by mechanical tolerancing of components.

6. STANDING WAVE POWER DENSITY

A further advantage of the crossed porro resonator is evident when the standing wave power density is compared to that in the normal resonator.

In figure 16 the intensities in various parts of the cavity are shown for a normal resonator and a crossed porro resonator. Neglecting losses the intensities are related by the following equations :

$$\text{Saturated gain} \quad G^2 (1 - T) = 1$$

$$\text{Output intensity} \quad I_{\text{out}} = T I_2$$

$$\text{and} \quad I_0 = I_2 (1 - T) = I_{\text{out}} (1 - T) / T$$

$$I_1 = G I_0 = I_{\text{out}} [\sqrt{(1 - T)}] / T$$

Using these, the normalised standing wave power density (SWPD) in the Q switch is for the normal configuration

$$\text{SWPD} = 2I_1 / I_{\text{out}} = [2\sqrt{(1 - T)}] / T$$

and for the crossed porro configuration

$$\text{SWPD} = 2 I_0 / I_{\text{out}} = 2 [(1 - T) / T]$$

The ratio of the SWPD (in the Q switch) for the crossed porro to that for the normal configuration is

$$\text{Relative SWPD} = \sqrt{(1 - T)}$$

For low coupling there is little difference, but for coupling in the usual range

$$\begin{array}{l} 50\% < T < 80\% \\ 70\% > \text{Rel. SWPD} > 45\% \end{array}$$

Hence the power density in the Q switch is significantly lower in the crossed porro configuration. This is particularly important where it is desired to use LiNbO_3 Q switches with their lower damage threshold.

7. SMOOTHING OF HOT SPOTS

In reference 13, it is pointed out that if the porro prism roof edges make an angle other than 90° then a ray is stepped around the laser rod progressively on each reflection from a porro prism. Figure 17 depicts an end on view of the laser rod showing the prism roof edges making an arbitrary angle θ . A ray starting at 0 reflects in prism 1 to position 1, down the rod to prism 2 then across prism 2 to position 2 and so on.

For the ray starting at 0, the azimuth angle is σ_0 , subsequent ray azimuth angles are given by the recurrence relations

$$\begin{aligned}\sigma_{2n} &= \sigma_0 - \alpha - n\theta \\ \sigma_{2n+1} &= -(\sigma_0 - 2\alpha - n\theta)\end{aligned}$$

The ray path will repeat itself if

$$\begin{aligned}\sigma_{2n} &= \sigma_{2m} + 2N\pi \\ \text{or} \quad \sigma_{2n+1} &= \sigma_{2m+1} + 2N\pi \\ \text{ie} \quad n' &= (n - m) = N(2\pi/\theta)\end{aligned}$$

If 2π is divisible by θ , $N = 1$. Thus when $\theta = 90^\circ$, $N = 1$ and $n' = 4$,

but for $\theta = 70^\circ$, $N = 7$ and $n' = 36$. Even when the porro prisms are nominally crossed it is unlikely the angle would be exactly 90° and some ray wandering would occur. At high repetition rates when thermal birefringence is present, causing local hot spotting, the effect of smoothing produced in this way could be of particular value.

8. CONCLUSION AND RECOMMENDATIONS

A detailed analysis of the mode of operation of the Crossed Porro Resonator has been performed. This has clarified a number of features of the design and shown an error in the presentation of the results of Chun and Teppo(ref.5).

The advantages of the design are

- 1) Easily adjustable output coupling.
- 2) No DC bias required on the Q switch for Nd:YAlG lasers operated below 100 mJ output level.
- 3) Some 30 times smaller sensitivity to mirror mis-alignment than in Fabry-Perot resonators.
- 4) Lower standing wave power density in the Q switch, allowing the use of LiNbO_3 .

- 5) Smoothing of hot spots by stepping the rays around in the rod.

The tolerances on the alignment of the prisms are such that it should only be necessary to provide tilt adjustment in the sensitive direction and rotation about the optical axis to adjust output coupling or biasing.

9. ACKNOWLEDGEMENTS

Thanks are due to Mr D. Bristow for design and fabrication of the optical mounts for the porro prisms and to Mr W. Schoff for assistance with the measurements.

REFERENCES

- | No. | Author | Title |
|-----|--|---|
| 1 | Control and Instrumentation Systems Group, Advanced Engineering Laboratories, DRCS | "Feasibility Study of an Airborne Laser Rangefinder for the Mirage III O." AEL-0062-SD |
| 2 | Buchman, W.W. | "Laser Q Switch Using a Roof Prism End Reflector and Electro-Optical Retarder." IEEE Journal of Quantum Electronics. QE1, Sept. 1965 |
| 3 | Podgaetskii, V.M. | "Application of the Jones Method for Computation of the Electrooptical-Shutter Characteristics in a Laser with Porro Prisms as Reflectors." Optics and Spectroscopy, 26, 153, 1969, pp153-155 |
| 4 | Chun, M.K. and Toppo, E.A. | "Laser Resonator : an Electrooptically Q-Switched Porro Prism Device." Applied Optics, 15, 8, Aug. 1976, pp1942-1946 |
| 5 | Ferranti, U.K. | UK Patent 1,358,023 |
| 6 | International Laser Systems. | US Patent 3,924,201 |
| 7 | Jenkins, F.A. and White, H.E. | Fundamentals of Optics, McGraw Hill, N.Y. 1957 |
| 8 | Born, M. and Wolf, E. | Principles of Optics, Pergamon Press, Oxford, 1965 |
| 9 | Shurcliffe, W.A. | Polarised Light, Harvard University Press, Cambridge, Mass. 1962 |
| 10 | Koechner, W. | Solid State Laser Engineering, Springer-Verlag, N.Y. 1976 |
| 11 | Mauer, P. | Phase Compensation of Total Internal Reflection. Journal of the Optical Society of America. 56, 9, Sep. 1966. pp1219-1221 |
| 12 | Kard, P.G. | On the Influence of Thin Films on Total Reflection. Optics and Spectroscopy. VI, 4, Apr. 1959 |
| 13 | Balin, B. Quentron Optics Pty.Ltd. | Evaluation of Nd:YAG Q-switched Laser Technology for Application to an Experimental Airborne Laser System |

APPENDIX I

THE JONES CALCULUS

An elliptically polarised light ray is shown in figure 18, this is represented by the vector

$$\begin{Bmatrix} A_x \exp(i \epsilon_x) \\ A_y \exp(i \epsilon_y) \end{Bmatrix}$$

where the intensity

$$I = \sqrt{ (A_x)^2 + (A_y)^2 }$$

The intensity is usually normalised to unity.

The relative phase $\gamma = \epsilon_x - \epsilon_y$

The angle $R = | \tan^{-1} (A_y/A_x) |$

The azimuth angle, the angle between the major axis and the horizontal, is

$$\begin{aligned} \alpha &= 1/2 \tan^{-1} (\tan 2R \cos \gamma), \text{ for } A_y/A_x < 1 \\ &= 1/2 \tan^{-1} (\tan 2R \cos \gamma) \pm \pi/2, \text{ for } A_y/A_x > 1 \end{aligned}$$

The ellipticity is

$$\beta = 1/2 \sin^{-1} (\sin 2R | \cos \gamma |)$$

and the ratio of semi-major to semi-minor axes is

$$b/a = \tan \beta$$

The result of passing a ray through a retarder is given by

$$\begin{Bmatrix} E_x \\ E_y \end{Bmatrix} = M \begin{Bmatrix} A_x \exp(i \epsilon_x) \\ A_y \exp(i \epsilon_y) \end{Bmatrix}$$

where M is a 2 X 2 matrix. For an ideal linear retarder of retardance δ , the phase shift matrix referred to the retarder axes is

$$P = \begin{Bmatrix} \exp(i \delta/2) & 0 \\ 0 & \exp(-i \delta/2) \end{Bmatrix}$$

If the retarder makes an azimuth angle ρ the matrix becomes

$$M = R(-\rho) P(\delta) R(\rho)$$

where $R(\rho)$ is the rotation matrix

$$R(\rho) = \begin{Bmatrix} \cos \rho & \sin \rho \\ -\sin \rho & \cos \rho \end{Bmatrix}$$

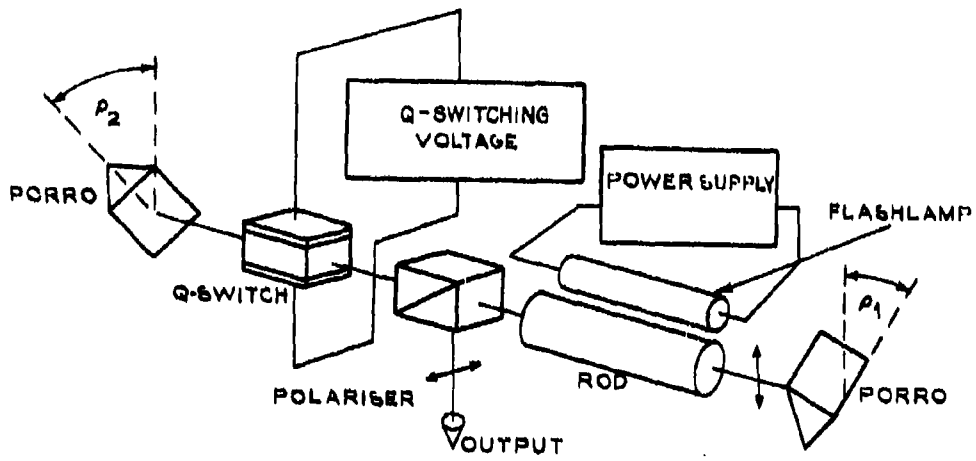
and M is then

$$M = \begin{Bmatrix} \cos \delta/2 + i \sin \delta/2 \cos 2\rho & i \sin \delta/2 \sin 2\rho \\ i \sin \delta/2 \sin 2\rho & \cos \delta/2 - i \sin \delta/2 \cos 2\rho \end{Bmatrix}$$

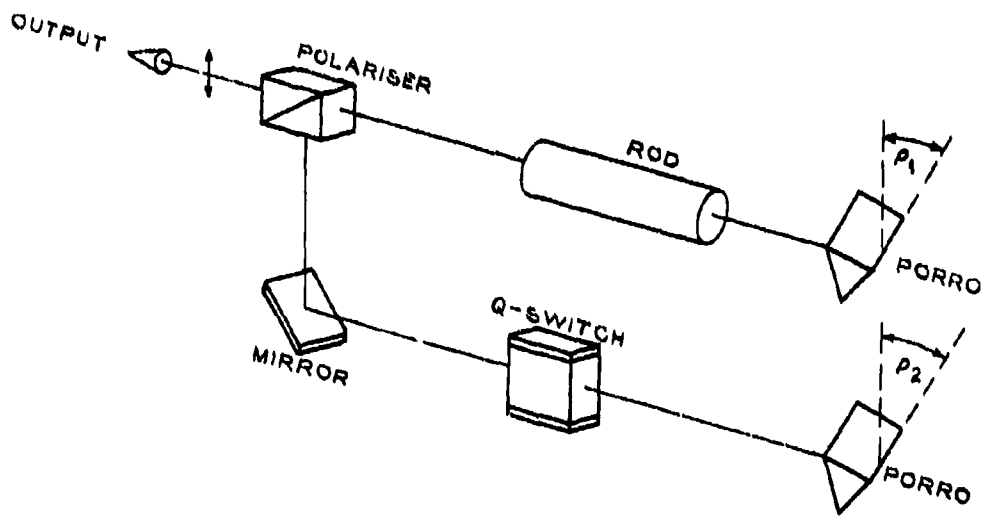
APPENDIX II

PROGRAM FOR TI 59
PHASE SHIFT, COUPLING AND EXTINCTION RATIO

Step	Instruction	Comments	Step	Instruction	Comments
004	2nd LBL A STO 00 R/S	n	070	RCL 02 2nd TAN	
009	2nd Lbl B STO 01 R/S	ρ_p	071	X	
014	2nd LBL C STO 09 R/S	$\delta\rho_p$	074	RCL 08 2nd SIN	
017	RCL 00 x^2		075	=	δ_q (open)
018	-		078	INV 2nd TAN	
019	2		081	-	
020	=		084	90	
021	$\sqrt{\quad}$		085	=	δ_q (shut)
022	+		086	STO 03 R/S	
025	RCL 00 =		089	2nd COS	
028	INV 2nd TAN		090	X	$\cos(\delta_p/2)\cos\delta_q$
029	X		095	STO 04 RCL 02	
030	4		096	2nd SIN	
031	=		099	X	
035	+		100	RCL 08 2nd SIN	
036	180		101	=	
037	=		104	X	
038	+		105	RCL 03 2nd SIN	
041	STO 02	$\delta_p/2$	108	=	$\sin(\delta_p/2)\sin(2\rho_p)\sin(\delta_q)$
042	R/S		111	STO 05 +	
044	RCL 01 +		112	RCL 04 =	$\cos(\delta_p/2)\cos(\delta_q)$ $+\sin(\delta_p/2)\sin(2\rho_p)\sin(\delta_q)$
047	RCL 09 =	$\rho_p + \Delta\rho_p$	117	x^2 STO 06	
050	STO 01 R/S		118	RCL 02 2nd SIN	
053	RCL 02 2nd SIN		121	X	
054	x^2		122	RCL 08 2nd COS	
055	X		125	=	$\sin(\delta_p/2)\cos(2\rho_p)$
056	(126	STO 07 x^2	
059	RCL 01 X		129	+	
060	2		130	RCL 06 x^2	
061)		131	=	$(A_y)^2$
064	STO 08 2nd SIN	$2\rho_p$	132	R/S	
065	x^2		133	1/x	
066	=		136	R/S	Ext. Ratio
067	R/S	Coupling		GTO 042	



1(a)



1(b)

Figure 1. In line and folded crossed porro resonators

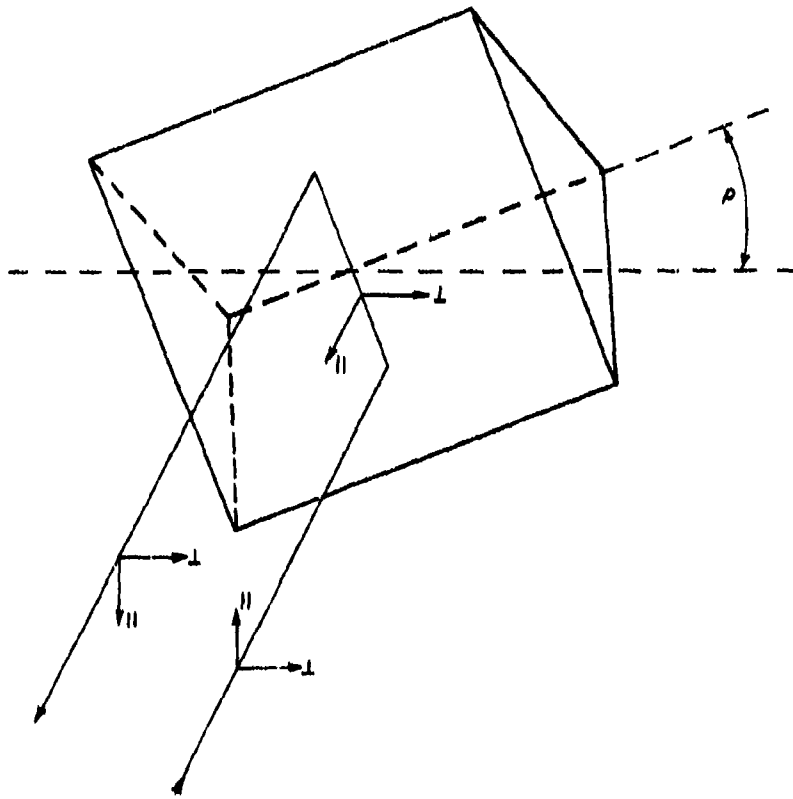


Figure 2. Reflection of light ray in a porro prism

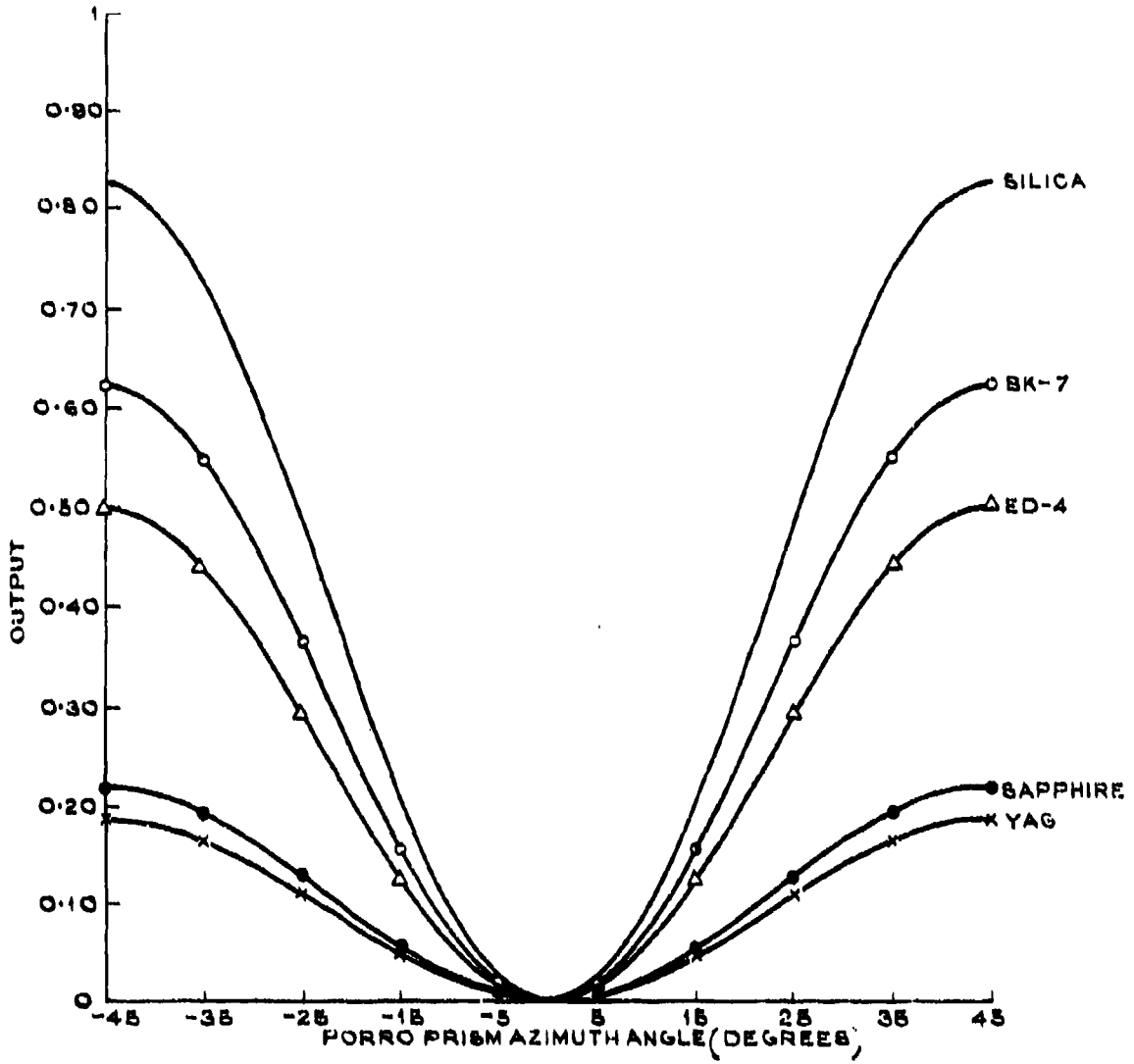


Figure 3. Output versus azimuth angle

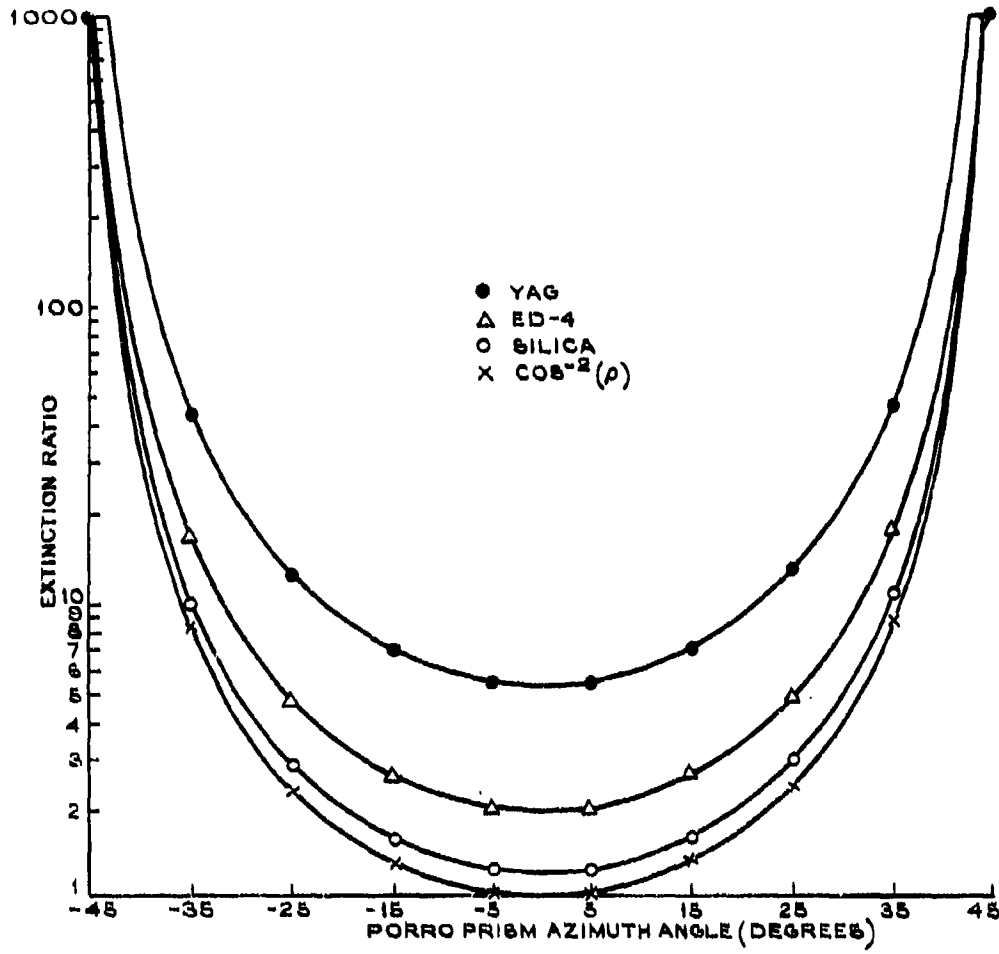


Figure 4. Extinction ratio with applied bias

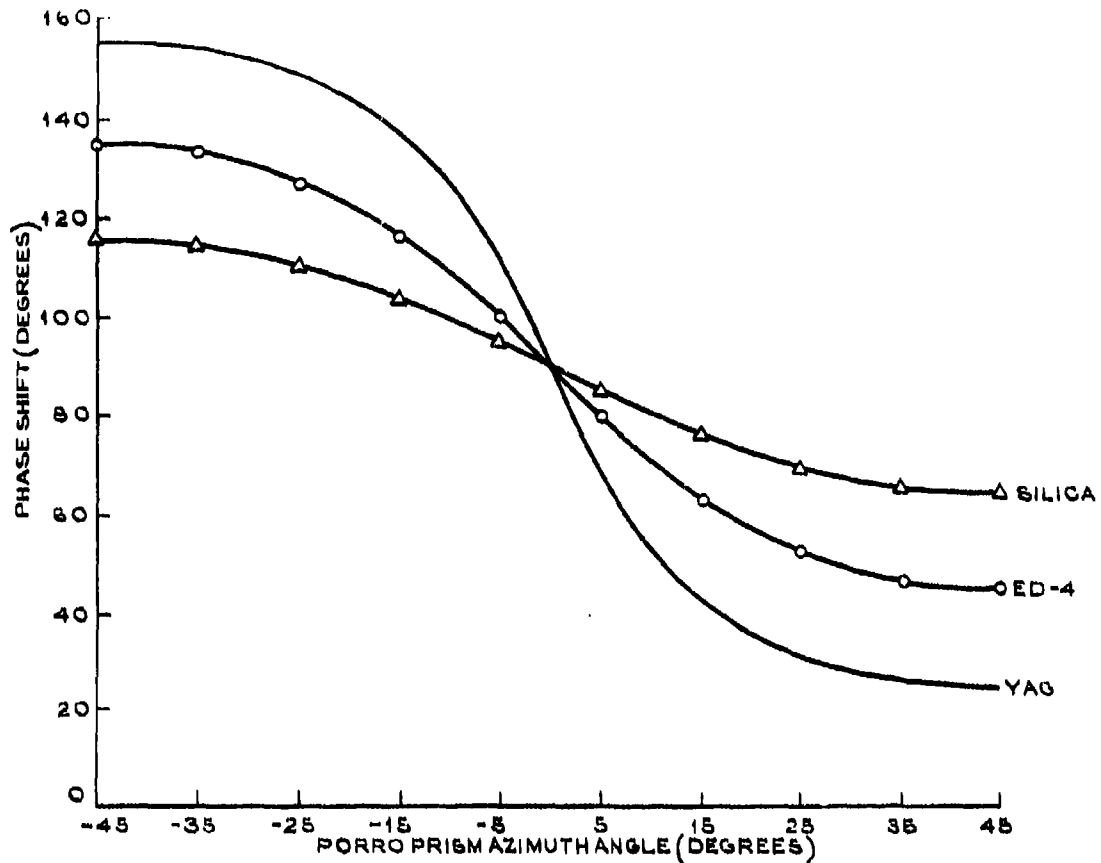


Figure 5. Phase shift to shut Q-switch

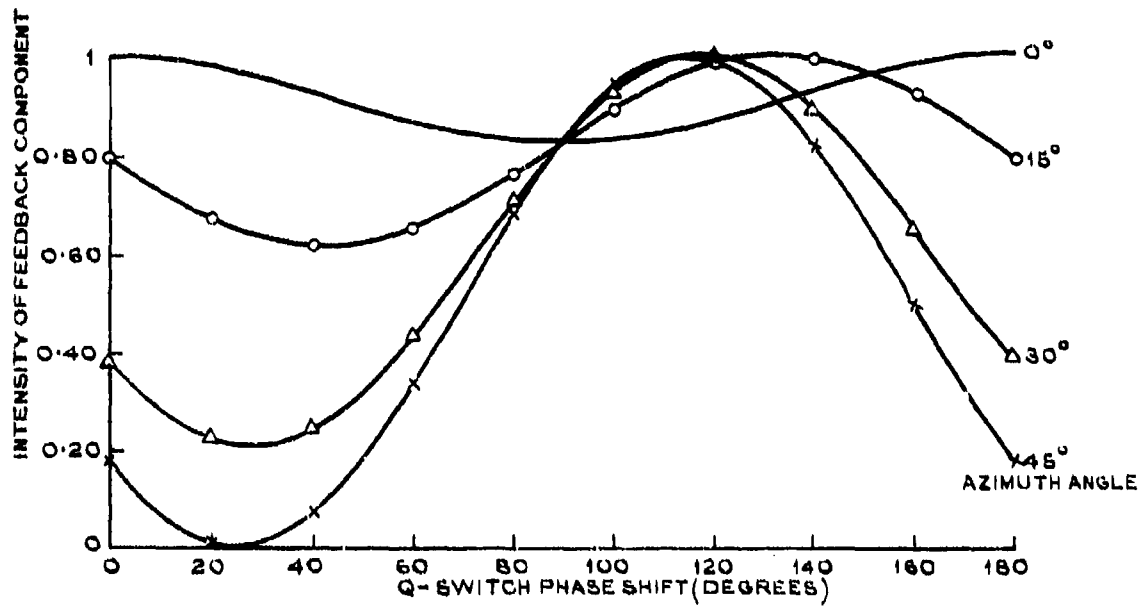


Figure 6. Feedback intensity vs. phase shift

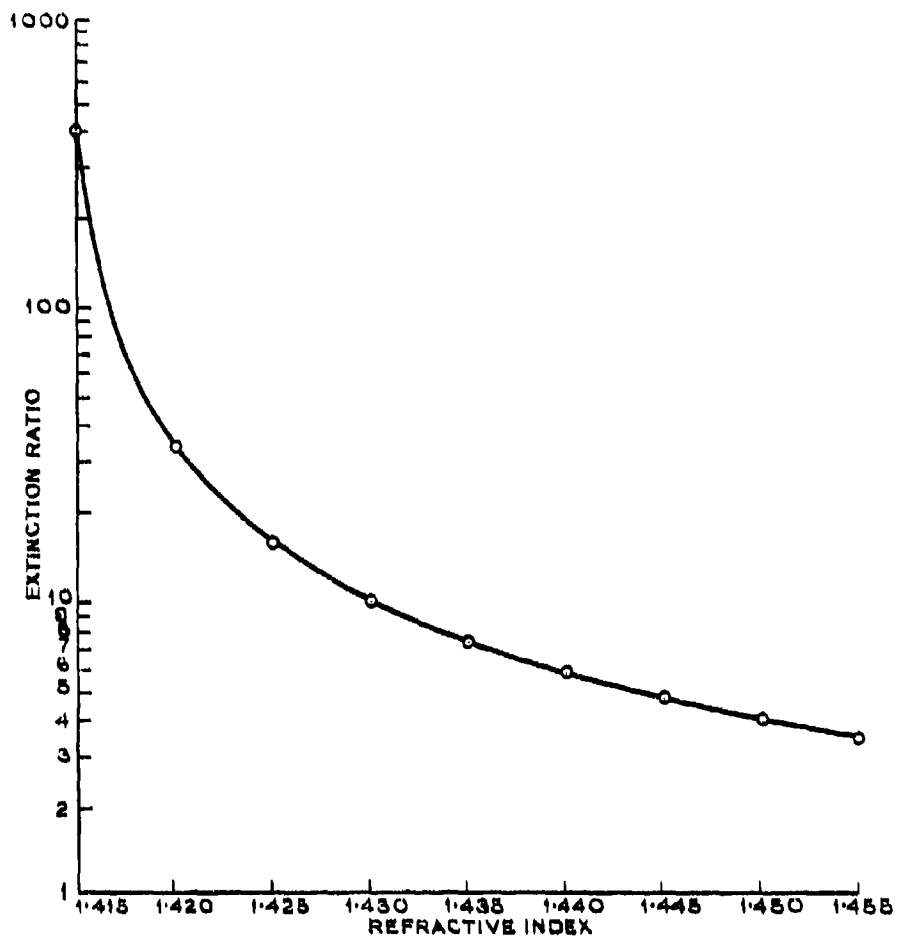


Figure 7. Extinction ratio vs. refractive index

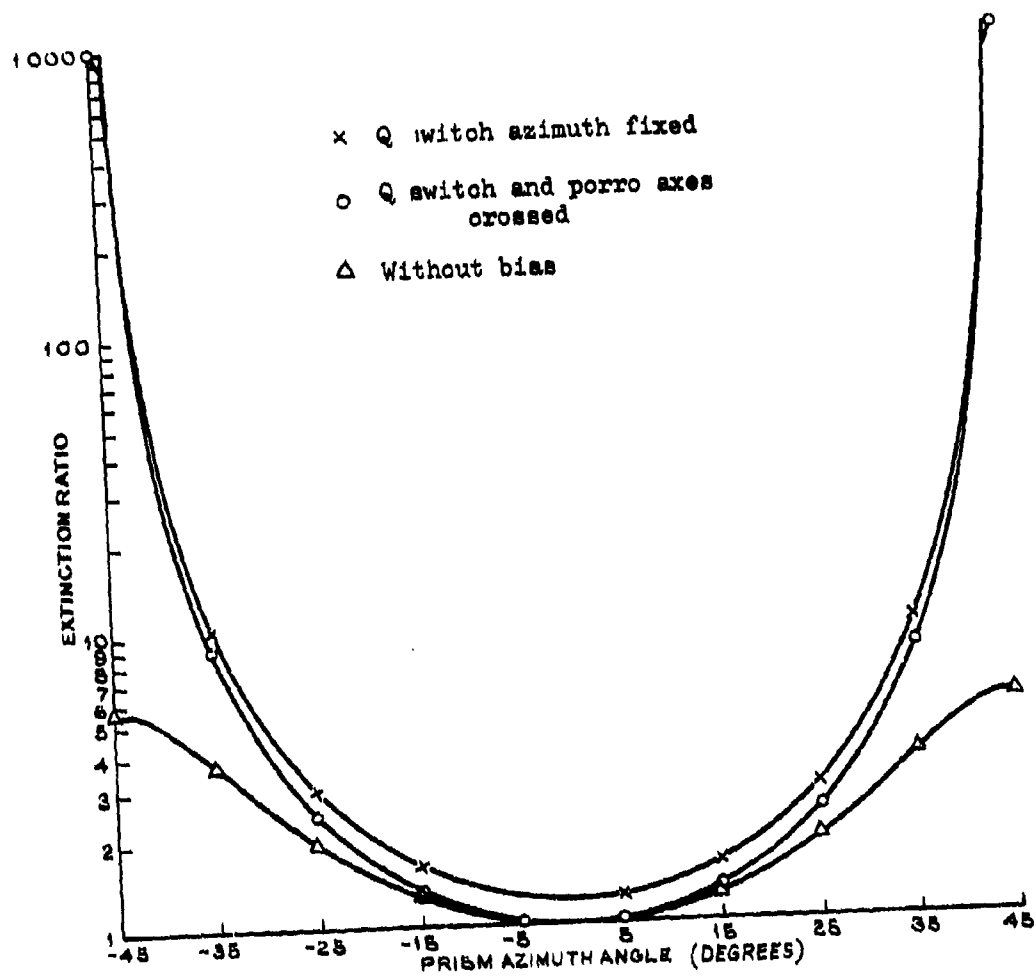


Figure 8. Extinction ratios for fused silica porro

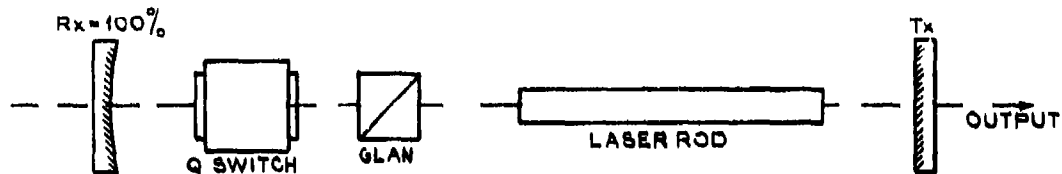
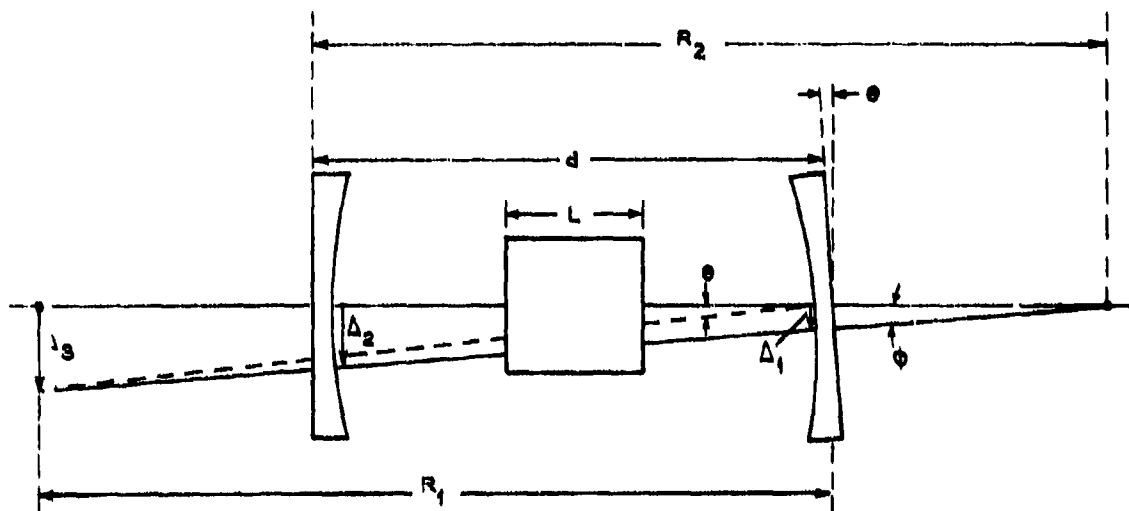
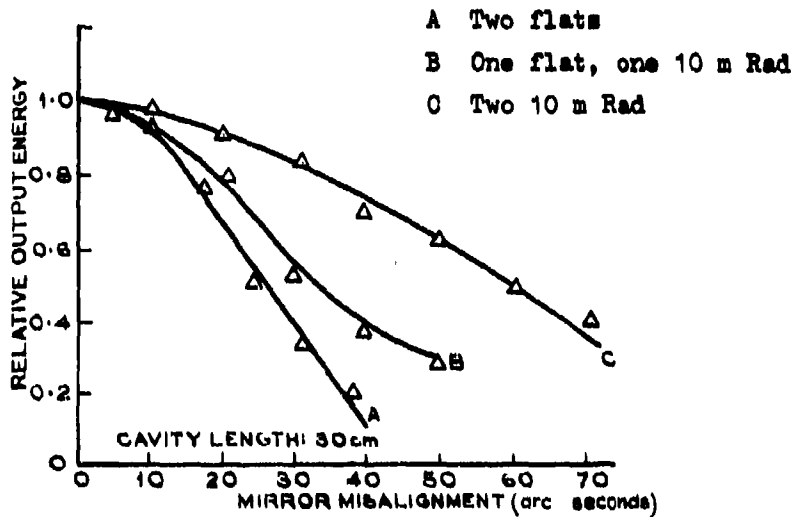


Figure 9. Conventional Fabry-Perot resonator



(a) Mirror Misalignment



(b) Output vs. Misalignment

Figure 10. Conventional resonator sensitivity

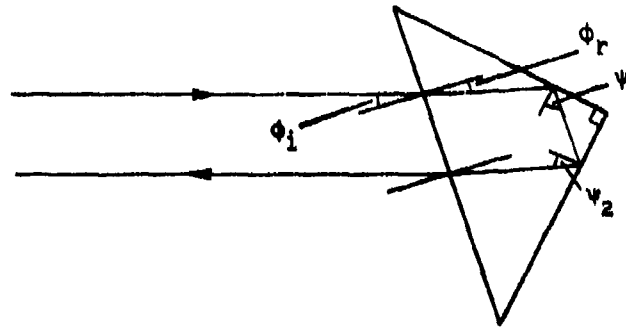


Figure 11. Porro prism tilted in its insensitive direction

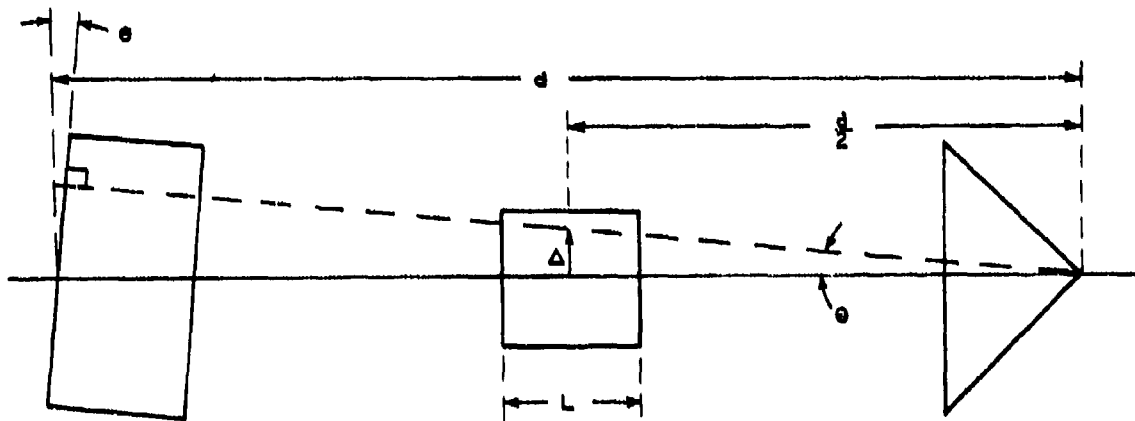
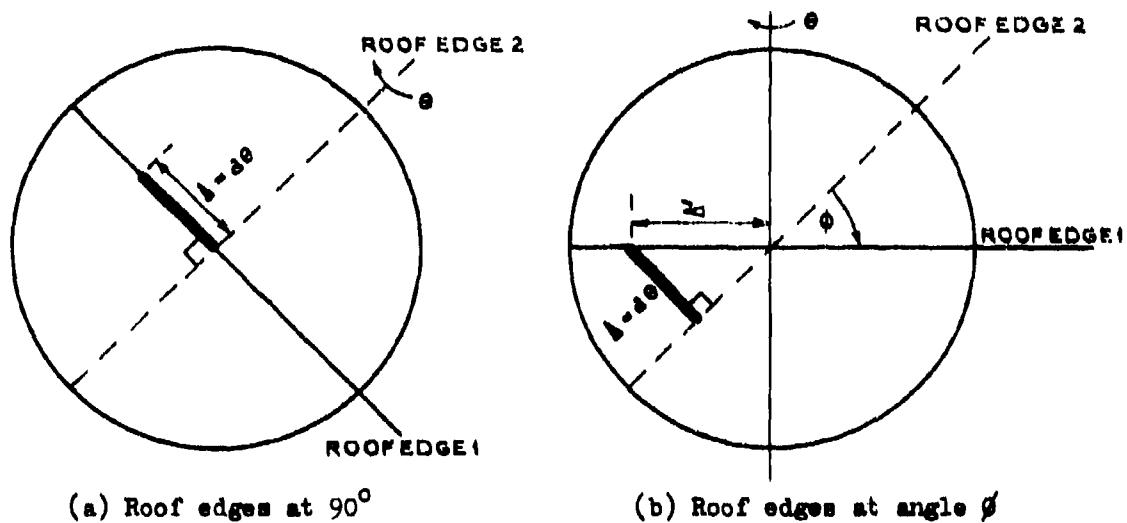


Figure 12. Porro prism tilted in its sensitive direction



(a) Roof edges at 90°

(b) Roof edges at angle ϕ

Figure 13. Projected view of optical axis displacement for porro prism

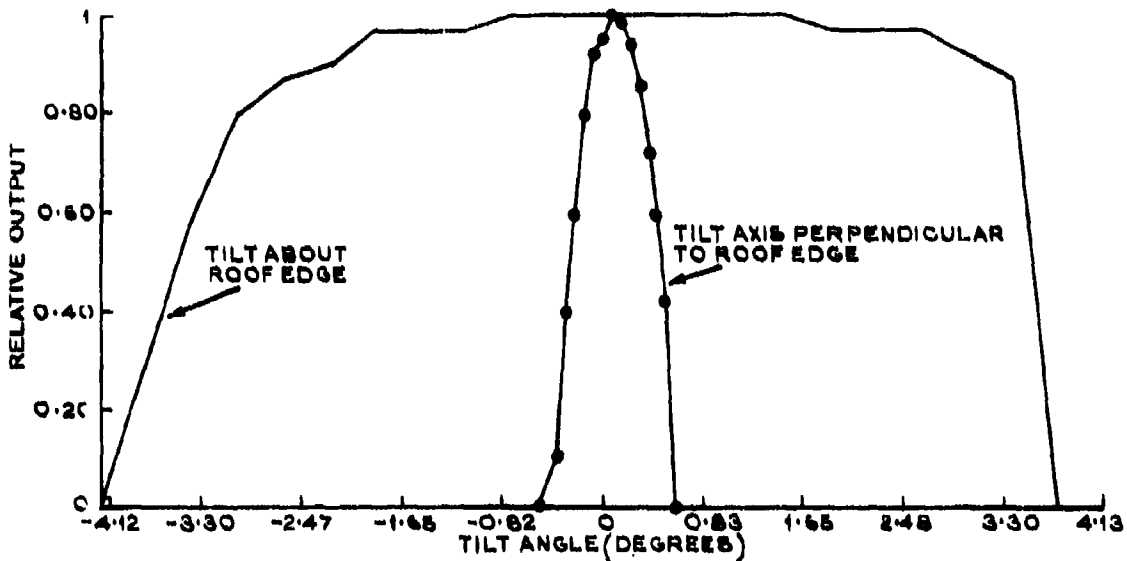


Figure 14. Relative output vs. porro misalignment

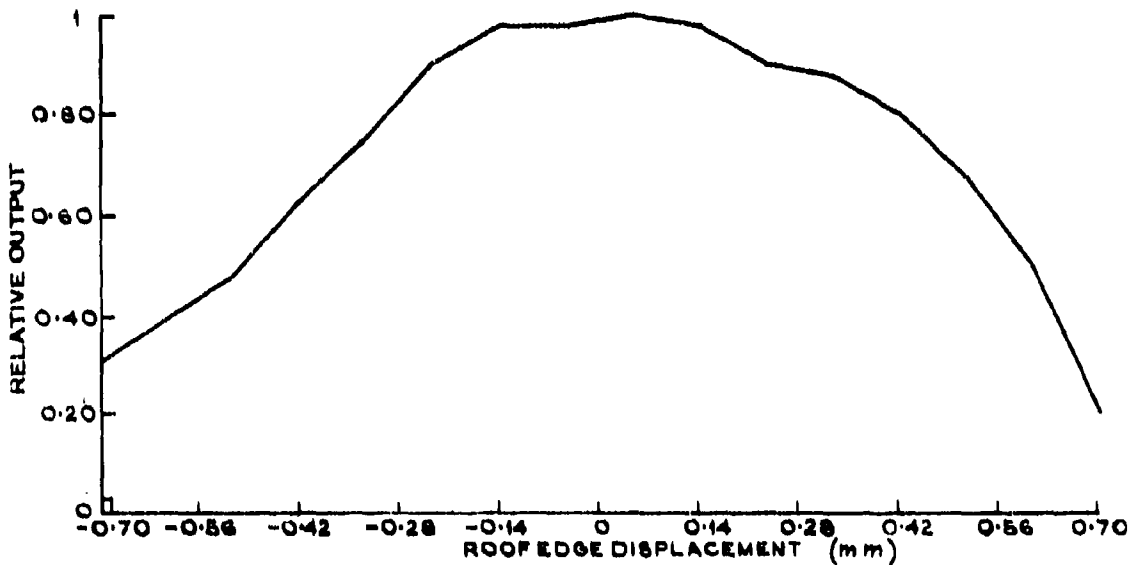
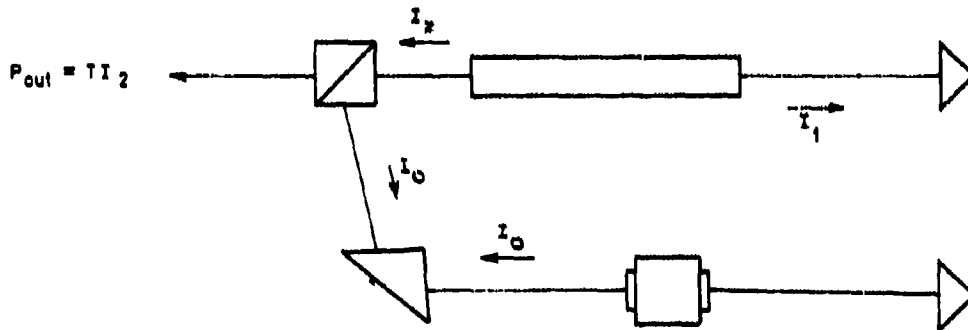


Figure 15. Relative output vs. roof edge displacement



(a) Fabry Perot resonator



(b) Folded crossed porro resonator

Figure 16. Beam intensities in resonators

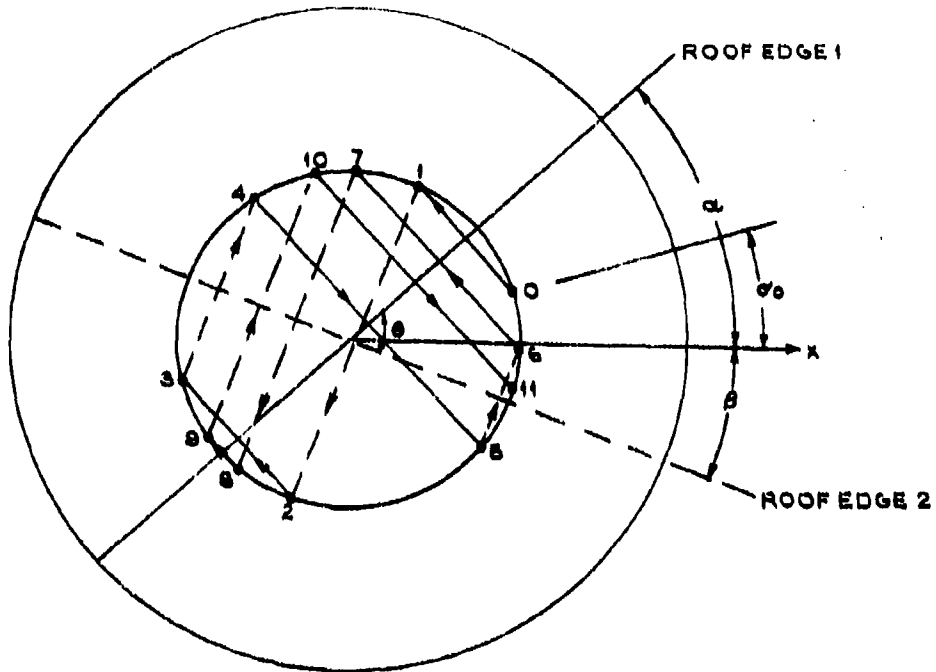


Figure 17. Ray path rotation in crossed porro resonator

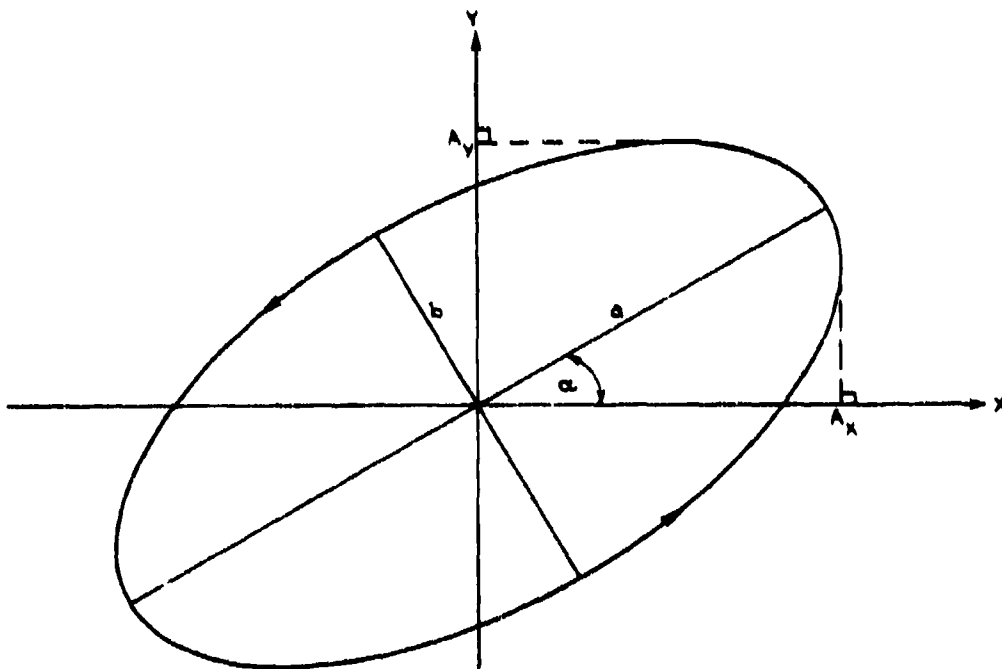


Figure 18. Elliptically polarised light ray

DISTRIBUTION

Copy No.

EXTERNAL

In United Kingdom

British Library Lending Division,
Boston Spa, Yorkshire 1

Technology Reports Centre, Orpington, Kent 2

In United States of America

National Technical Information Service,
Springfield, Va. 3

NASA Scientific and Technical Information Office,
Washington DC 4

In Australia

Chief Defence Scientist 5

Deputy Chief Defence Scientist 6

Controller, Projects and Analytical Studies 7

Superintendent, Major Projects 8

Superintendent, Science and Technology Programmes 9

Defence Information Services Branch (for microfilming) 10

Defence Information Services for:

United Kingdom, Ministry of Defence,
Defence Research Information Centre (DRIC) 11

United States, Department of Defense,
Defense Documentation Center 12 - 23

Canada, Department of National Defence
Defence Science Information Service 24

New Zealand, Ministry of Defence 25

Australia National Library 26

Defence Library, Campbell Park 27

Library, Aeronautical Research Laboratory 28

Library, Materials Research Laboratory 29

Director, Joint Intelligence Organisation (DDST1) 30

WITHIN DRCS

Chief Superintendent, Electronics Research Laboratory 31

Superintendent, Navigation and Surveillance Division	32
SPRS Surveillance, Mr J.R. Pyle	33
Principal Officer, Laser Group	34
Principal Officer, Optical Techniques Group	35
Principal Officer, Terminal Guidance Group	36
Principal Officer, Control and Instrumentation Systems Group	37
Principal Officer, Mechanisms and Instrumentation Group	38
Mr M.F. Penny, Laser Group	39
Mr C. Lowe, Terminal Guidance Group	40
Dr J. Richards, Laser Group	41
Dr D. Phillips, Laser Group	42
Mr D. Rees, Laser Group	43
Mr P. Wilsen, Laser Group	44
Mr C. Lightowler, Control and Instrumentation Systems Group	45
Mr N. Irwin, Terminal Guidance Group	46
Authors	47 - 52
Library	53 - 54
Spares	55 - 58

The official documents produced by the Laboratories of the Defence Research Centre Salisbury are issued in one of five categories: Reports, Technical Reports, Technical Memoranda, Manuals and Specifications. The purpose of the latter two categories is self-evident, with the other three categories being used for the following purposes:

- Reports** : documents prepared for managerial purposes.
- Technical Reports** : records of scientific and technical work of a permanent value intended for other scientists and technologists working in the field.
- Technical Memoranda** : intended primarily for disseminating information within the DSTO. They are usually tentative in nature and reflect the personal views of the author.